INDIAN JOURNAL OF SCIENCE AND TECHNOLOGY

RESEARCH ARTICLE

Robust Analysis of Dual Rotor Radial Flux Induction Motor Used for Industrial Application

Chetan M Bobade[1,2]*, Swapnil B Mohod[3], S K Singh[4]

1 Research Scholar, Prof. Ram Meghe College of Engineering & Management, Badnera, Amravati, Maharashtra, India
2 Head of Department, Department of Electrical Engineering, G H Raisoni University, Amravati, Maharashtra, India
3 Professor and Dean IQAC, Department of Electrical Engineering, Prof. Ram Meghe College of Engineering & Management, Badnera, Amravati, Maharashtra, India
4 Professor, School of Digital Technology, Atlas SkillTech University, Mumbai, Maharashtra, India

OPEN ACCESS

Received: 28-10-2023
Accepted: 07-01-2024
Published: 31-01-2024

Citation: Bobade CM, Mohod SB, Singh SK (2024) Robust Analysis of Dual Rotor Radial Flux Induction Motor Used for Industrial Application. Indian Journal of Science and Technology 17(5): 457-464. https://doi.org/10.17485/IJST/v17i5.2719

* **Corresponding author**.

bobade.cm@gmail.com

Funding: None

Competing Interests: None

Published By Indian Society for Education and Environment (iSee)

ISSN
Print: 0974-6846
Electronic: 0974-5645

Abstract

Background: Dual Rotor Radial Flux Induction Motor (DRRFIM) is proposed in this study to improve the operating performance in a more concise way for several applications compared to the conventional Induction motor. Mathematical analyses are obtained from the modeling and analytical study of Double Rotor Induction Motors (DRIM) which are useful to determine the dynamical behavior of the motor in saturated and unsaturated conditions. **Methods:** In normal DRIM, the driving state flow equation is done by the state equations in q-d axis and Park's transformation. To develop and design such models, it is advised to use better optimization techniques adapted MATLAB2020/Simulink software for validation. Further, transient, and steady state performance of the DRRFIM is analyzed in the various scenarios with and without saturation in DRRFIM. **Finding:** The proposed research also compares conventional IM with optimization possibilities. In addition, a DRIM is being operated at different stages of load connectivity and the level of speed conditions is being further investigated in this work. The method proposed and implemented in this paper achieved the overall efficiency is 82% by optimizing the mention performance metrics like active and reactive power of machine, speed of motor and its torque performance. **Novelty and Applications:** Dynamical behavior of solving and optimizing the amplitude of unsaturated and saturated magnetic flux are of utmost importance. The study also presents a machine equipped with two rotors that uplift the performance of the induction motor. This machine has the potential to be utilized in industrially important applications as well as in vehicles that are driven by electricity.

Keywords: Dual Rotor RadialFlux Induction Motor (DRRFIM); Saturation; Unsaturation; Mathematical Model; Inner and Outer Rotor

1 Introduction

The raising effectiveness of induction motor during recent years result in severe energy savings. Many researchers have already intended to refine and enhance the efficiency of induction motors in this respect. Further, the efficiency of induction motors can be enhanced by providing better cooling mechanisms, materials, and by developing electromagnetic stability. Theoretically, the concept of a induction machine includes the twin rotors which is characterized by both outer and inner rotors [1]. There are few current trends or advancements related to dual-rotor induction motors which are not often used in industrial applications. Constant research in the industry for DRIM helps to increase electric motor efficiency. Various research in the core materials, robust designs, and control algorithms for twin-rotor induction motors help to minimize energy losses as well [2,3].

On the other hand, use of variable-speed drives, such as twin-rotor induction motors, has the potential to improve system management which increases energy efficiency. The progression of power electronics and control systems has resulted in enhanced sophistication and adaptability of the available system [4,5]. DRIM has unique benefits that make it suitable for use in wind turbines and other renewable energy sources. As the production of renewable energy grows, there can be advances in this field. The enhancement of performance and grid integration of DRIM may be achieved via the development of sophisticated control algorithms. The characteristics include predictive maintenance, condition monitoring, and grid synchronization.

Several research universities and institutions are often at the forefront of motor technology research. They are conducting experiments or prototyping new motor configurations, including dual rotor designs. Research may be focused on optimizing the electromagnetic design of these motors to achieve better performance including torque characteristics and power factor control [3]. DRIM has other potentials to affect the grid stability in power production applications, such as wind farms. Research in grid integration and control methods may have impactful significance. DRIMs are used in some applications of hybrid electric vehicles. The automotive sector is now seeing a notable shift towards hybrid and electric cars, which is expected to significantly influence advancements in this domain [6–10]. The major contributions of the proposed paper are-

- To develop the steady state and dynamical model for a Modified Dual Rotor Induction Motor.
- To simulate and design Dual Rotor Induction Motor using MATLAB2020.
- Comparative evaluation of DRIM in saturation and unsaturated condition with recently reported works.

2 Methodology

2.1 Working Principle of Double Rotor Induction Machine (DRIM)

This section gives a quick description of the DRIM's structure and principles to help us to learn more about modelling. In terms of construction, the DRIM varies greatly from common induction motors. This system's stator layout is unusual, and the rotors are squirrel cages. The outer rotor is protected by a cylindrical casing whereas the stator conductors are positioned in teeth and slots on both the internal and external sides of the DRRFIM stator. Internal and external rotors are physically interconnected here. Figure 1 depicts the Rotor and Stator structure of conventional DRIM.

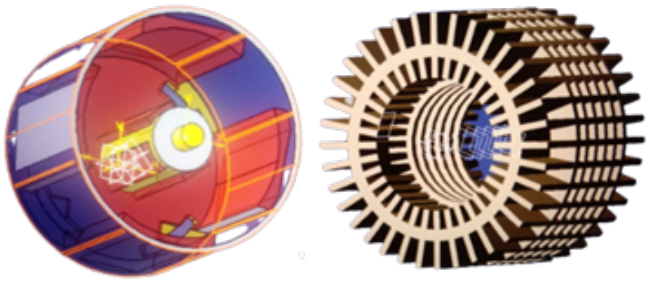

Fig 1. Rotor and Stator structure of DRIM [1–3]

In terms of service, the DRIM is identical to Induction Machines. A three-phase symmetrical current runs through the coils of the stator, they form a rotational magnetic flux. The magnetic field is divided into two directions that move across air gaps and rotors. In accordance with Lenz's Law, the windings of the generator induced current due to the counteraction of the revolving stator magnetic field against the movement of rotor-winding currents. This interaction propels the rotor to revolve along with the trajectory rotor of the revolving magnetic field of the stator. The rotor will keep rotating until the torque and induced rotor

current are equal to the applied load.

The end winding conductor's length is notably shortened compared to a normal induction motor. Consequently, the resistance and leakage inductance of the DRRFIM stator winding are reduced to those of traditional induction motors. For improved analysis, the DRIMs' performance, reliability, and power factor are improved. The function improves the DRIM's performance, reliability, and power factor. However, when two or four-pole DRIM is used, the leakage inductances of the stator winding are decreased to 71.5-81.5% of those reported in common induction motors. The aforementioned decrease results in a notable gain in both the performance and power factor of the DRRFIM, surpassing 3.5% and 0.083, respectively, as reported in [9].

2.2 Analysis of Magnetic Fields

To simplify magnetic research on the DRRFIM, the core magnetic permeability is assumed to be infinite, and the core failure is ignored. Figure 2 illustrates that clarify magnetic equivalent circuit for the DRIM's building upon the foundation. Magnetic reluctance between the internal rotor and the stationary stator itself is represented as Irm, while the magnetic reluctance between the outer rotor and the stator is denoted as Orm. The turn numbers for the windings of internal and external rotors, external rotors and stators are represented as Nrti, Nrto, and Nst respectively. Self and reciprocal inductances are denoted by (1) - (4) as a result (4).

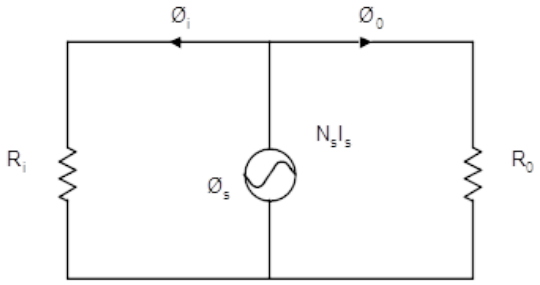

Fig 2. The DRIM'S Equivalent Magnetic Circuit

$$L_s = N^2 (P_o - P_i) = L_{ss,o} + L_{ss,i} \tag{1}$$

$$L_{sro} = L_{ros} = N_{st} N_{rto} P_o \tag{2}$$

$$L_{sri} = L_{ris} = N_{st} N_{rti} P_i \tag{3}$$

$$L_o = N_{rto}^2 P_o,\ L_i = N_{rti}^2 P_i \tag{4}$$

Where $P_o$and P_i are equivalent to $\frac{1}{R_o}$ and $\frac{1}{R_i}$, respectively and

L_s : Stator own inductance of DRIM.

L_o *and* L_i : Outer and inner rotors own-inductances of DRIM.

L_{sro} : Common (Mutual) inductance between both the stator and the outer rotor min.

L_{sri} :Common (Mutual) inductance between both the stator and the inner rotor maximum value.

Rotor positioning affects the mutual inductance between rotors and stators. To ensure the optimum performance of the DRRFIM, it's essential to adjust the lengths of the air gaps to achieve the best power density. The distribution of magnetic flux is most favorable when the difference in air gaps between the outer and inner rotors is equal, as this configuration results in the highest power density[2,3].

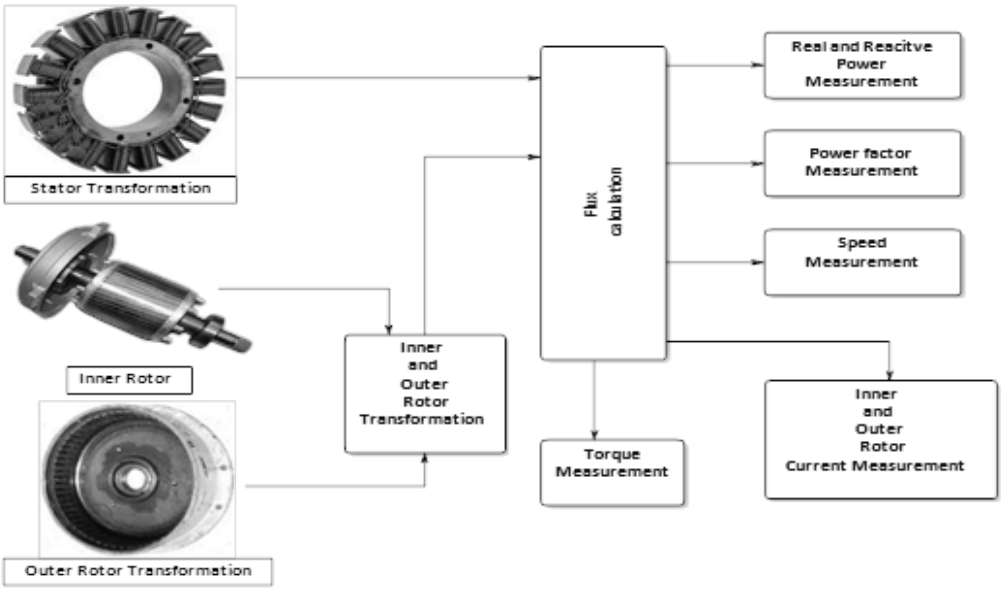

Fig 3. Proposed Block Diagram of Induction Motor

To assess the effects of saturation on DRIM, DRRFIM's efficiency has been studied under various speed and load conditions. Torque, RPM, currents (Amp) in the stator winding and rotor winding, real and reactive power, performance, PF, and torque-RPM performance characteristic are all included in the simulation results. Table 1 summarizes the specifications for the motor used. The findings of dual rotor induction motor simulation model are presented in detail. In no load condition the torque of 20 N-m is provided to the unit at time setting t=2. The load torque is decreased by fifty percent when time setting at t=4. Figure 5 depicts the electromotive Torque (T), rpm, and current parameters of both rotor and stator. It can be further demonstrated that as the load torque goes up, the stator current down while the motor speed (rpm) decreases, and the motor torque (Tm) matches the load torque (Tl). When the load torque is drop, the current of stator down and the speed of the motor rises. Figure 5 indicates the effects of variation in load of the current of both rotor and stator[5]. The magnitude and frequency of the rotor currents rises as the burden is added to the DRIM at time setting of 2, approaching a steady state value. Since the load is instantly decreased current magnitude and frequency drop. The real and reactive strength, performance, PF, and torque-RPM performance characteristics are shown in Figure 4 at time setting of 4.

Table 1. Rated Parameter of Induction Motor

Sr. No	Symbol (S)	Details Parameter (P')	Value (V)
1	P	Total number of Poles	4
2	P_rated	Rated output power in watts	4 kW
3	T_rated	Rated torque (N-m)	20 NM
4	V_rated	Rated LL voltage	310-320 V
5	Js_rated	Rated frequency of stator (Hz)	50 Hz
6	Rs	Stator resistance	0.82
7	Rri	Internal rotor resistance	0.602
8	Rro	Outer rotor resistance	0.1 .2
9	Lmi	Magnetizing inductance between stator and Internal rotor	0.18 H
10	Lmo	Magnetizing inductance between stator and External rotor	0.21 H
11	Lis	Stator leakage inductance	0.002 H
12	Liri	Internal rotor leakage inductance	0.0015 H
13	Liro	External rotor leakage inductance	0.00101 H
14	J	inertia Rotor	0.18 KGm^2

2.3 Dynamic Modeling of DRIM

The instantaneous increase in voltages across the stator and rotors can be described using the fifth equation in the matrix.

$$[V1] = [R][i] + \frac{d}{dt}[\lambda], \ [\lambda] = [i] \tag{5}$$

Voltage and current vectors, as well as the resistance matrix, are represented by [V], [I]and [R], respectively.

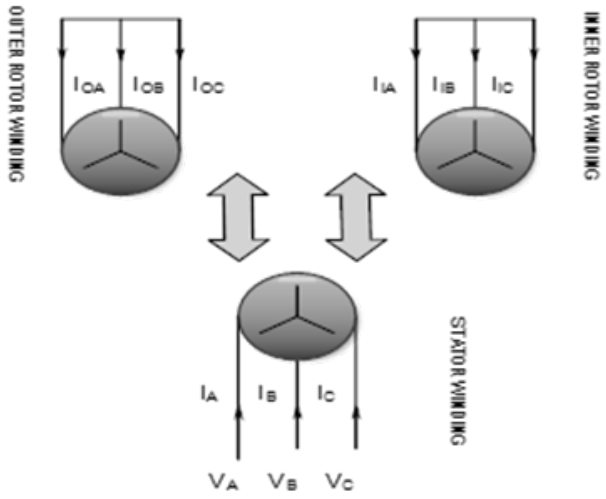

Fig 4. Dual Rotor Induction Motor winding structure

The voltage vectors of the internal and external rotors are both zero due to the occurrence of short-circuited at the end rings of the rotors. [Ro], [Rst] and [Ri] denote the resistances of the sandwich stator, external rotor, and internal rotor, correspondingly. The utilization of the finite element analysis (FEM) method enables the computation of the aforementioned inductance values (Lsro, Lsri, Lsm, and so on) because θrk = rk t + θr k0 (k = i,o) varies with rotor position, the matrix component's [Lso] and [Lsi] should be considered time variable parameters[11–14].

2.4 Effects Saturation in the Machine Model

The DRRFIM has two common (mutual) flux links, one among the stator and External rotor (om) and the other among the stator and internal rotor (ir), due to its unique winding and configuration (im). Depending on the design, composition, and size of the internal and exterior rotors as well as the air gap length, both shared fluxes may become saturated. The difference (Gap) in amplitudes of magnetizing fluxes saturated and unsaturated, as shown in Figure 5, is used in this paper's DRRFIM model to provide magnetizing flux saturation. The unsaturated and saturated flux linkages on the d-q axes are linked by-

$$\begin{cases} \psi_{q,om}^{Sat} = \psi_{q,om}^{Sat} - \triangle\psi_{q,om} \\ \psi_{d,om}^{Sat} = \psi_{d,om}^{Sat} - \triangle\psi_{d,om} \end{cases} \tag{6}$$

$$\begin{cases} \psi_{q,im}^{Sat} = \psi_{q,im}^{Sat} - \triangle\psi_{q,im} \\ \psi_{d,im}^{Sat} = \psi_{d,im}^{Sat} - \triangle\psi_{d,im} \end{cases} \tag{7}$$

The not equal (gap) in the size of the unsaturated and saturated magnetizing fluxes of the outside air gap is represented by the terms $\Delta\psi_{d,om}$, and $\Delta\psi_{q,om}$. In a similar vein, the inner air distance is connected to both $\Delta\psi_{d,im}$ and $\Delta\psi_{q,im}$.

3 Result and Discussion

The current study attempts to increase the machine's performance parameters (active power, reactive power, motor speed and torque performance, and power factor) up to the level of 82%. By monitoring efficiency, control, power factor, active and reactive power, the overall system's motor performance and power density are improved shown in Tables 2 and 3.

Table 2. Representation of DRRFIM with Saturated and Unsaturated Condition

Parameter	Stator Current	Rotor Current		Power		Power Factor	Efficiency
Speed 1800 Rpm		Inner	Outer	Active	Reactive		
Saturated	Ist saturated = 4.5 Amp	Ii = 2.5 Amp	Io = 2.5 Amp	P = 100 W	Q = 170 var	8.6	86%
Unsaturated	Ist unsaturated = 5 Amp	Ii = 2.15 Amp	Io = 2.1 Amp	P = 200 W	Q = 160 var	8.2	82%

Table 3. Performance Parameters at Variable Speed Condition

Speed in RPM	Torque	Active power	Reactive Power
1200	30 N-m	P = 200 W	Q = 100 Var
1400	36.3 N-m	P =178 W	Q =125 Var
1600	42 N-m	P = 167 W	Q = 142 Var
1800	49.5 N-m	P = 102 W	Q = 165 Var

In this section, the simulation results of DRIMs under varying speeds achieved by simultaneous adjustments in voltage and frequency while maintaining a constant V/f ratio. Specifically, it is reduced to a voltage from 310 V to 205 V which decreases the frequency from 50 Hz to 40 Hz, all while keeping a steady load torque of 20 N-m (normal load). Figure 5 illustrates the key findings of this analysis, presenting a comprehensive view of the motor's performance characteristics under different speed conditions. First, Figure 5**(a, b, c)** displays the DRIM's speed variations, highlighting the motor's response to changes in voltage and frequency. This adjustment helps to minimize starting torque, demonstrating the motor's adaptability to variable operating conditions. Additionally, Figure 5 provides insights into the motor's electrical behavior. It showcases active power, reactive power, motor performance, and power factor across the range of speeds. These parameters are critical for assessing the motor's efficiency, power factor correction, and overall operational suitability.

In summary, the simulation results emphasize the DRIM's ability to maintain performance and adapt to varying different speed conditions by adjusting voltage (Volts) and frequency (Hz) while ensuring a stable V/f ratio. Additionally, the analysis of active power, reactive power, motor performance, and power factor offers a comprehensive understanding of the motor's behavior under different operational settings, providing valuable insights for motor control and optimization strategies.

3.1 Saturated and Unsaturated DRRFIM Correlation

The simulation model is designed to investigate the impact of saturation on the output of the DRIM under conditions of equal saturation and no saturation. This examination aims to understand how saturation affects the motor's performance when subjected to a constant load torque of Tl = 20 N-m. Figure 6 provides a comprehensive representation of the simulation results, displaying electromagnetic torque, RPM (revolutions per minute), stator current, and rotor current in both the saturated and unsaturated cases. Figure 6 **(a)** clearly demonstrates that the DRIM's starting torque is higher compared to the saturated case. This highlights the saturation effect, which reduces the motor's initial torque output.

Moreover, the saturated DRIM exhibits a longer starting time (as evident in Figure 6**(b)**, indicating that it takes more time to accelerate and reach its final speed compared to the unsaturated counterpart. This delay is a consequence of the saturation factor's influence on the motor's response. Examining the stator current, shown in Figure 6**(c)**, we observe a notable difference between the saturated and unsaturated various cases. In the saturated case, the stator current exhibits a considerable rise during startup due to the saturation effect, while the unsaturated case shows a more stable current profile. Additionally, Figure 6 **(d)** illustrates the behavior of rotor current in both scenarios. Notably, in the saturated case, the starting torque is reduced, leading to a more stable rotor current profile compared to the unsaturated case, where the initial torque is higher, resulting in a more fluctuating rotor current. In conclusion, these simulation results clearly demonstrate the significant influence of saturation on the DRIM's performance. Saturation reduces the starting torque, prolongs the startup time, and affects the stator and rotor current profiles. Understanding these effects is crucial for optimizing the operation of DRIMs under various load conditions and saturation levels, offering valuable insights into motor control and design considerations.

Figure 6 also provides a comprehensive view of the Dual Rotor Induction Motor's (DRIM) performance characteristics under both saturated and unsaturated conditions. This analysis covers active and reactive power, motor performance, power factor, and the torque-speed relationship. In the saturated scenario, shown in Figure 6**(g)** and **(h)**, there is a noticeable increase in both

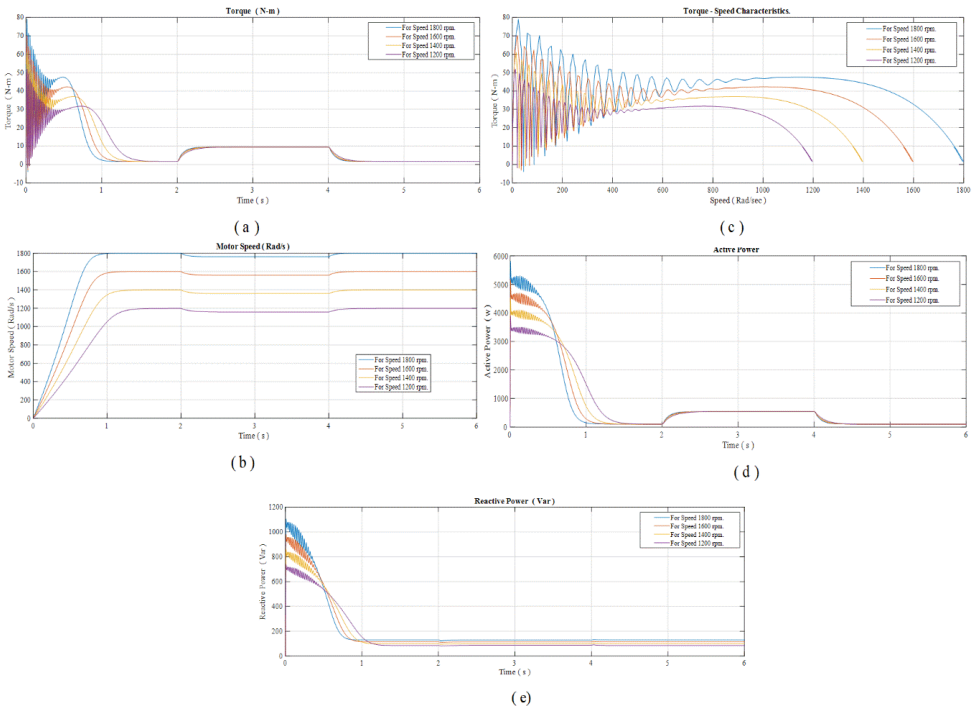

Fig 5. (a) Plot of Electromagnetic Torque, (b) Speed, (c) Torque Speed. (e) Active Power, (d) Reactive Power

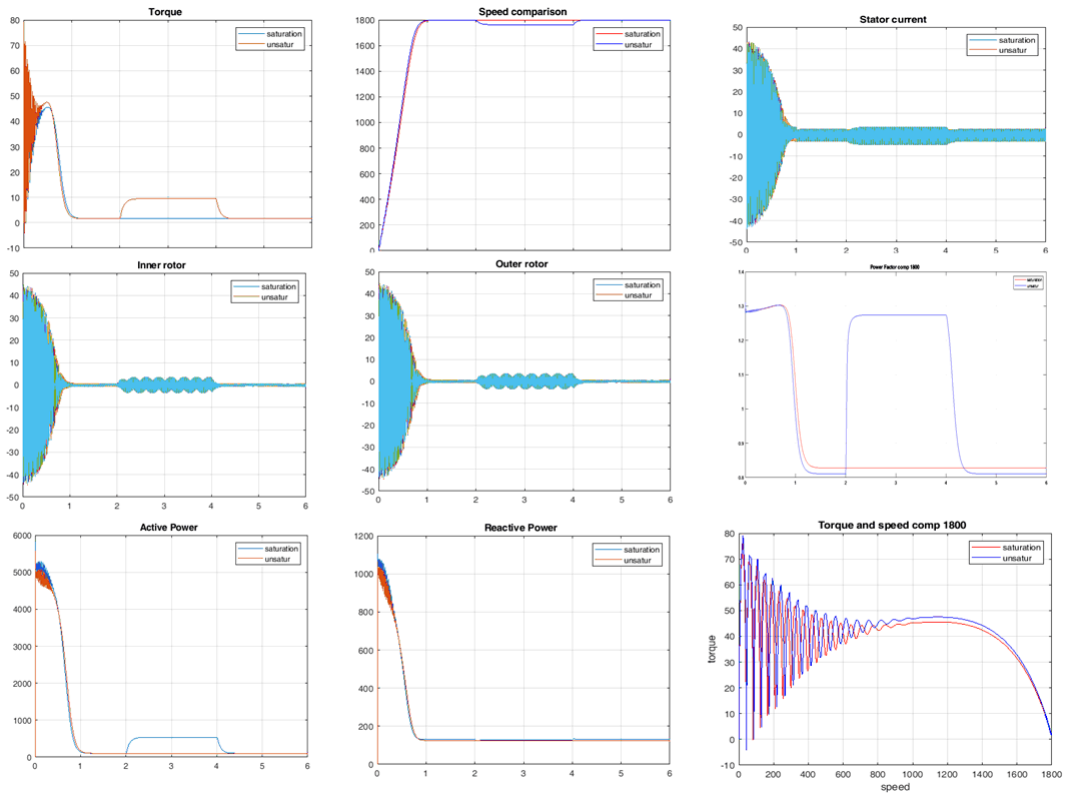

Fig 6. Plot of (a) Electromagnetic Torque, (b) Speed, (c) Stator Current, (d,e) Inner And Outer Rotors Currents Saturated and Unsaturated Condition (f) Power Factor (g,h) Active and Reactive Power and (i) Torque vs Speed Curve

active and reactive power consumption by the motor. Interestingly, the increase in reactive power is even more pronounced than that of active power. Consequently, the power factor observed in the saturated state (Figure 6**(f)** is lower compared to the unsaturated condition. This decrease in power factor significantly impacts the DRIM's overall efficiency, resulting in decreased efficiency levels when the motor operates in a saturated state. Furthermore, Figure 6 **(i)** illustrates another critical observation: the starting torque of the DRIM is notably reduced under saturation conditions. This reduction in starting torque highlights the influence of saturation on the motor's initial performance. In summary, these findings underscore the significant impact of saturation on various performance metrics of the DRIM. It results in increased power consumption, a drop in power factor, reduced efficiency, and lower starting torque. Understanding these effects is essential for optimizing the operation and control of DRIMs in practical applications.

4 Conclusion

In the present study, a basic model of a Dual Rotor Radial Flux Induction Machine (DRRFIM) with and without saturation in magnetic field is studied and presented to investigate the behavior in steady-state and transient. The saturation of magnetizing fluxes is taken into consideration in the DRRFIM model by comparing the amplitudes of magnetizing flux, unsaturated and saturated magnetizing flux. The equation related to mathematical modelling of the both mechanical and electrical sections of the DRIM's outlined in the q-d axis state equations are utilized to create this model. The recommended models are also utilized to study the special effects of saturated effect, skin effect, load variations, and variation in speed on DRIM functioning. The simulation findings reveal that the suggested model can reflect the DRIM's transient and steady-state behaviors. Furthermore, future DRIM research may be created while taking into consideration the model's minor aspects.

5 Acknowledgement

The authors thank the researchers who contributed to the field of Dual Rotor Induction Motor that motivated us to work in this field. Authors also thank Prof. Ram Meghe College of Engineering & Management, Badnera, Amravati, Sant Gadge Baba Amravati University and G H Raisoni University, Amravati for providing the required technical support for performing the experiments.

References

1) Li Y, Bobba D, Sarlioglu B. Design and optimization of a novel dual-rotor hybrid PM machine for traction application. *IEEE Transactions on Industrial Electronics* . 2018;65(2):1762–1771. Available from: https://doi.org/10.1109/TIE.2017.2739686.
2) Kahourzade S, Mahmoudi A, Roshandel E, Cao Z. Optimal design of Axial-Flux Induction Motors based on an improved analytical model. *Energy*. 2021;237:121552. Available from: https://doi.org/10.1016/j.energy.2021.121552.
3) Al-Ani M. Multi-physics design and analyses of dual rotor synchronous reluctance machine. *eTransportation*. 2021;8:100113. Available from: https://doi.org/10.1016/j.etran.2021.100113.
4) Zhang X, Zhang B. Analysis of Magnetic Forces in Axial-Flux Permanent-Magnet Motors with Rotor Eccentricity. *Mathematical Problems in Engineering*. 2021;2021:1–8. Available from: https://doi.org/10.1155/2021/7683715.
5) Yang SH, Pyo HJ, Jung DH, Kim WH. A Study on Optimal Design Process of Dual Rotor Axial-Flux Permanent Magnet Synchronous Motors. *Machines*. 2023;11(4):1–18. Available from: https://doi.org/10.3390/machines11040445.
6) Kumar RR, Devi P, Chetri C, Kumari A, Saikia PM, Saket RK, et al. Performance analysis of dual stator six-phase embedded-pole permanent magnet synchronous motor for electric vehicle application. *IET Electrical Systems in Transportation*. 2023;13(1):1–13. Available from: https://doi.org/10.1049/els2.12063.
7) Siddiqi MR, Yazdan T, Im JH, Humza M, Hur J. Design and Analysis of a Dual Airgap Radial Flux Permanent Magnet Vernier Machine with Yokeless Rotor. *Energies*. 2021;14(8):1–15. Available from: https://doi.org/10.3390/en14082311.
8) Dalal A, Kumar P. Design, Prototyping, and Testing of a Dual-Rotor Motor for Electric Vehicle Application. *IEEE Transactions on Industrial Electronics*. 2018;65(9):7185–7192. Available from: https://doi.org/10.1109/TIE.2018.2795586.
9) Omran KC, Mosallanejad A. Modeling and simulation of saturated double rotor induction machine. *COMPEL - The international journal for computation and mathematics in electrical and electronic engineering*. 2018;37(3):1139–1165. Available from: https://doi.org/10.1108/COMPEL-05-2017-0221.
10) Golovanov D, Galassini A, Flanagan L, Gerada D, Xu Z, Gerada C. Dual-Rotor Permanent Magnet Motor for Electric Superbike. In: 2019 IEEE International Electric Machines & Drives Conference (IEMDC). IEEE. 2019;p. 951–956. Available from: https://doi.org/10.1109/IEMDC.2019.8785287.
11) Wang P, Shi L. Analysis of a Novel Dual-Rotor Induction Motor for Pulsed Power Driving System. *IEEE Access*. 2019;7:154818–154826. Available from: https://doi.org/10.1109/ACCESS.2019.2948951.
12) Nobahari1 A, Darabi A, Hassannia A. Various skewing arrangements and relative position of dual rotor of an axial flux induction motor, modelling and performance evaluation. *IET Electr Power Appl*. 2018;12(4):575–580. Available from: https://doi.org/10.1049/iet-epa.2017.0716.
13) Soheili P, Darabi A, Deylami FP. Design and modelling of a two-degrees-of-freedom dual-rotor axial-flux squirrel cage induction motor. *IET Electric Power Applications*. 2023;17(9):1159–1169. Available from: https://doi.org/10.1049/elp2.12331.
14) Kahourzade S, Mahmoudi A, Roshandel E, Cao Z. Optimal design of Axial-Flux Induction Motors based on an improved analytical model. *Energy*. 2021;237:121552. Available from: https://doi.org/10.1016/j.energy.2021.121552.